Biophysical Chemistry 9 (1979) 313–328
© North-Holland Publishing Company

SCANNING MOLECULAR SIEVE CHROMATOGRAPHY OF INTERACTING PROTEIN SYSTEMS. III. EFFECT OF KINETIC PARAMETERS ON THE LARGE ZONE BOUNDARY PROFILES FOR LOCAL EQUILIBRATION BETWEEN MOBILE AND STATIONARY PHASES ☆

Paul W. CHUN ‡ and Mark C.K. YANG ‡‡

Department of Biochemistry and Molecular Biology, College of Medicine, University of Florida, Gainesville, Florida 32610, USA

Received 15 February 1978

Large zone reaction boundary profiles for molecular sieve chromatography as affected by kinetic parameters have been simulated for local equilibration between the mobile and stationary phases. Our studies of monomer–dimer and monomer–tetramer systems indicate that in a slowly equilibrating system, the kinetic controls operating between the mobile and stationary phases contribute most significantly to the overall boundary profile. In a rapidly equilibrating system, however, the kinetic parameters k_{ij} and k_{ji} operating in the mobile phase are the principal determinants of the reaction boundary, while the kinetic effects of k_{ii} and k_{-ii} between the mobile and stationary phases are minimal.

1. Introduction

Transport processes such as scanning molecular sieve chromatography [1–8] have proven a useful complement to ordinary ultracentrifugal equilibrium techniques in defining the nature of a chemical reaction for self-associating systems, in which a chemically reacting solute can impart a great deal of information about the solute and the reactions in which it participates.

Since no methods exist to date which make it possible to infer directly the nature of a solute and its interactions from the boundary profile, a number of computer simulation procedures have been developed, using finite difference models of the transport process to predict the boundary profiles that will be given by various interacting systems [9–21]. Zimmerman and Ackers [22] have used the simulation technique to predict the behavior of a number of rapidly equilibrating systems on various chromatographic media [22–27]. Zimmerman [25] has expanded this simulation procedure to consider an entire range of chemical reaction rates, from infinitely rapid to infinitely slow, under kinetic control. These earlier simulation techniques [22–27], however, have been limited to consideration of the interacting species distribution in a rapidly equilibrating system.

We have recently reported, from computer simulation studies, that the slope and development of the reaction boundary for the chemically interacting species in a self-associating system, a function of the equilibration time along the gel column length is influenced by the effective kinetic rate of local equilibration between mobile and stationary phases [15]. The solute partition cross-section and axial dispersion operator of such an interacting protein system under kinetic control have been simulated by [1] time discretization, [2] the finite difference approximation of Fick's second law [14] and [3] the kinetic expression for the concentration of monomer $C^*_{1(t)}$ as a function of equilibration time [15].

In our examination of the effect of kinetic controls, we have found that although the chemical reaction rate for cases of rapid equilibration in the mobile phase

☆ This work was supported by NSF Grant PCM 76-04367 and, in part, by the University of Florida Computer Center.
‡ Address correspondence to P.W. Chun, Department of Biochemistry and Molecular Biology, College of Medicine, Box J-245, JHMHC, University of Florida, Gainesville, FL. 32610.
‡‡ Department of Statistics, College of Arts and Sciences, University of Florida, Gainesville, FL.

is the principal determinant of the shape of the elution boundary, the kinetically-controlled reaction rate between mobile and stationary phases is the principal perturbing factor of the reaction boundary. Hence, decreasing the rate of equilibration in the mobile phase has a much greater effect on the shape of the boundary profile in molecular sieve chromatography than does decreasing the rate of equilibration between phases [15].

The most significant overall finding of these computer-simulated gel permeation experiments is that the kinetically-controlled effects of local equilibration along the column in either the mobile or stationary phase influence the apparent equilibrium constant as a function of the distance coordinate. The concentration gradient profiles vary when evaluated for each species at each point along the column between the mobile and stationary phases.

In this communication, we report on the computer simulation of the continuity equation for chromatographic transport [3,28] as applied to distribution of monomer as a function of equilibration time, $C_{1(t)}$, between the mobile and stationary phases, for various types of self-associating systems. These results are compared with the $C^*_{i(t)}$ distribution in the mobile phase alone. Although previous simulation techniques have considered the column equilibrium coefficient for a given self-associating species to be constant, we have found that this varies as a result of kinetic effects.

2. Basic quantities for simulation of the gradient boundary profile of the large zone experiments

The expression for an idealized chromatographic continuity equation for the exchange of solute between the stationary and mobile phases is

$$\frac{\partial C_i^*}{\partial t} = \frac{L_i \partial^2 C_i^*}{\partial X} - \frac{F}{\xi_i}\frac{\partial C_i^*}{\partial X} - \sum_{j\neq i} k_{ij}(C_i^*)^j + \sum_{j\neq i} k_{ji}(C_j^*)^i - k_{-ii}C_i^* + k_{ii}C_i^{**}, \quad (1)$$

where k_{ij} is the chemical reaction rate from species i to j and C_i^* and C_i^{**} are the concentration of species i in the mobile and stationary phase, respectively. The

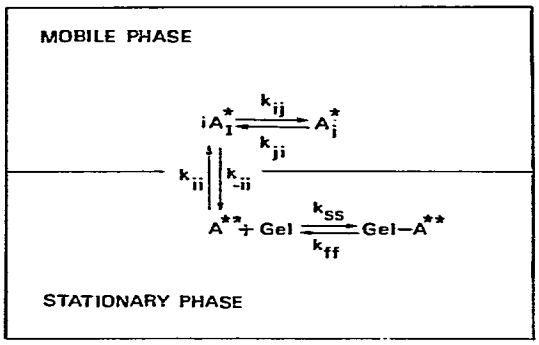

Fig. 1. A simplified model for solute association in the mobile and stationary phase in the gel column [15].

$\{-\Sigma_{j\neq i} k_{ij}(C_i^*)^j + \Sigma_{j\neq i} k_{ji}(C_j^*)^i\}$ term represents a local equilibration in the mobile phase and $(-k_{-ii}C_i^* + k_{ii}C_i^{**})$ represents an equilibration between the mobile and stationary phases. F is the elution flow rate, ξ_i is the solute partition cross-section, $\xi_i = (F/A)(dt/d\bar{x})$ and L_i is the axial dispersion coefficient characteristic of solute turbulence within the gel matrix.

In considering a monomer–$n$mer system, i.e. $nA_1^* \underset{k_{n1}}{\overset{k_{1n}}{\rightleftharpoons}} A_n^*$, then the kinetic expression for the concentration of monomer, $C_{1(t)}^*$, as a function of equilibration time in the mobile phase, as shown in fig. 1, becomes

$$dC_{1(t)}^*/dt = -k_{1n}[C_{1(t)}^*]^n + k_{n1}[C_{n(t)}^*], \quad (2)$$

$$dC_{n(t)}^*/dt = -dC_{1(t)}^*/dt,$$

where $C_{1(t)}^* + C_{n(t)}^* = C_T^*$ is the total concentration, a constant. Hence the differential equation (2) becomes

$$dC_{1(t)}^*/dt = -k_{1n}[C_{1(t)}^*]^n - k_{n1}C_{1(t)}^* + k_{n1}C_T^*. \quad (3)$$

As in eq. (1), we consider first only these solute molecules which begin to flow through the column under two initial boundary conditions in the state of A* in the mobile phase, in order to determine the species distribution of monomer as a function of time, $C_{1(t)}^*$. These distributions are then compared with distribution patterns showing the kinetic effect on the monomeric species equilibrium between the mobile and stationary phases.

The initial boundary conditions [15] to be consider-

ed here are (i) at $t = 0$, $C^*_{1(t)} = 0$ and (ii) at $t = 0$, $C^*_{1(t)} = C^*_T$.

The reaction is assumed to be pseudo first order kinetics. In our simulation, we assume that A**, the concentration of the stationary phase, contributes less significantly to binding to the gel matrix than does

$$A^{**} + \text{gel} \underset{k_{ff}}{\overset{k_{ss}}{\rightleftharpoons}} \text{gel} \sim A^{**}$$

the axial dispersion.

The general kinetic expressions for the concentration of monomer as a function of equilibration time, $C^*_{1(t)}$, in the mobile phase for various types of self-associating systems become:

(I) $n = 1$, isomerization:
$dC^*_1/\{[k_{1n} + k_{n1}]C^*_1 - k_{n1}C^*_T\} = -dt$,
(II) $n = 2$, monomer–dimer system:
$dC^*_1/\{k_{1n}(C^*_1)^2 + k_{n1}C^*_1 - k_{n1}C^*_T\} = -dt$,
(III) $n = 3$, monomer–trimer system:
$dC^*_1/\{k_{1n}(C^*_1)^3 + k_{n1}C^*_1 - k_{n1}C^*_T\} = -dt$,
(IV) $n = 4$, monomer–tetramer system:
$dC^*_1/\{k_{1n}(C^*_1)^4 + k_{n1}C^*_1 - k_{n1}C^*_T\} = -dt$. (4)

I) In the evaluation of $C^*_{1(t)}$ and the equilibrium constants as a function of column length for a self-associating protein system involved in a reversible isomerization between $A^*_1 \underset{k_{n1}}{\overset{k_{1n}}{\rightleftharpoons}} a^*_1$, the formation of the analytical solution is similar to that of Halvorson and Ackers [27], i.e.

(i): $t = 0$, $C^*_{1(t)} = 0$, then

$$C^*_{1(t)} = \left[\frac{k_{n1}}{(k_{1n} + k_{n1})}\right] C^*_T\{1 - \exp[-(k_{1n} + k_{n1})t]\}$$

(ii): $t = 0$, $C^*_{1(t)} = C^*_T$, then

$$C^*_{1(t)} = C^*_T - \left[\frac{k_{1n}}{(k_{n1} + k_{1n})}\right] \times C^*_T\{1 - \exp[-(k_{1n} + k_{n1})t]\}. \quad (5)$$

Here the development of the reaction boundary as a function of column length is influenced by the kinetic rate of local equilibration of $C^*_{1(t)}$ in the mobile phase.

II) For two-species association, a monomer–dimer system when $n = 2$, the quantity $C^*_{1(t)}$ under these boundary conditions,

(i): at $t = 0$, $C^*_{1(t)} = 0$

(ii): at $t = 0$, $C^*_{1(t)} = C^*_T$, is found to be

$$C^*_{1(t)} = \frac{\lambda}{2k_{1n}} \frac{k_0 - e^{-\lambda y'}}{k_0 + e^{-\lambda t}} - \frac{k_{n1}}{2k_{1n}}, \quad (6)$$

where $\lambda = (k^2_{n1} + 4k_{1n}k_{n1}C^*_T)^{1/2}$ and k_0 depends on the initial condition $C^*_{1(0)}$, and may be expressed as

$$\frac{\lambda + k_{n1} + 2k_{1n}C^*_{1(0)}}{\lambda - k_{n1} - 2k_{1n}C^*_{1(0)}} = k_0. \quad (7)$$

To this point, the evaluation of $C^*_{1(t)}$ in terms of kinetic constants is a simple matter, and will suffice to evaluate the monomer distribution within the local gel bed. Although it might be considered advantageous to consider an expanded set of boundary conditions for an infinite gel column bed, this would nullify the simple, exact solution of the general kinetic expression made possible under the stringent boundary conditions we have imposed.

III) For a monomer–trimer system where $n = 3$, the solution to eq. (4) is complicated by the necessity of considering an algebraic power series. Hence, we must solve the generalized kinetic expression by setting up a series of quadratic equations. In general kinetic terms, eq. (4) becomes

$$dC^*_1/[(C^*_1)^3 + Q(C^*_1) - QC^*_T] = -k_{1n}dt, \quad (8)$$

where $Q = (k_{n1}/k_{1n}) = 1/K$. Thus, K is the equilibrium constant in the mobile phase. Letting $C^*_1 = x$, and

$$a = QC^*_T/2 + [(QC^*_T)^2/4 + Q^3/27]^{1/2}, \quad \alpha = a^{1/3},$$

$$b = QC^*_T/2 - [(QC^*_T)^2/4 + Q^3/27]^{1/2}, \quad \beta = b^{1/3},$$

substitution of these quantities into eq. (8) yields

$$x^3 + Qx - QC^*_T = (x - P)(x^2 + Px + q), \quad (9)$$

where $P = (\alpha + \beta)$ and $q = \alpha^2 + \beta^2 - \alpha\beta$. Letting $Q = 1/(q + 2P^2)$, eq. (9) becomes

$$\frac{1}{(x - P)(x^2 + Px + q)} = \frac{Q}{(x - P)} - \frac{Q(x + 2P)}{(x^2 + Px + q)}. \quad (10)$$

Thus, eq. (9) may be solved by setting up the following equation.

$$\log|x-P| - \tfrac{1}{2}\log|x^2+Px+q| - \frac{3P}{2}\frac{1}{|\alpha-\beta|}\tan^{-1}\left(\frac{2x+P}{|\alpha-\beta|}\right) = -\frac{k_{1n}}{Q}t + k_0. \quad (11)$$

Assuming the initial boundary conditions

(i) $t = 0$, $C^*_{1(t)} = 0$, then the analytical solution for eq. (11) will determine $C^*_{1(t)}$, where

$$k_0 = \log(P/\sqrt{q}) - \frac{3P}{|\alpha-\beta|}\tan^{-1}\left(\frac{P}{|\alpha-\beta|}\right). \quad (11a)$$

(ii) $t = 0$, $C^*_{1(t)} = C^*_T$, then

$$k_0 = \log(C^*_T - P) - \tfrac{1}{2}\log[(C^*_T)^2 + PC^*_T + q] - \frac{3P}{|\alpha-\beta|}\tan^{-1}\left(\frac{2C^*_T+P}{|\alpha-\beta|}\right). \quad (11b)$$

The quantity k_0 is known, given the concentration C^*_T and the previously defined values of p, q, α and β. Hence, eq. (11) can be solved for $C^*_{1(t)}$ under either set of boundary conditions.

IV) For a monomer–tetramer associating system, where $n = 4$, a general biquadratic equation must be set up to solve the general kinetic expression in eq. (4) by considering two quadratic functions, simultaneously. The general kinetic expression is as follows:

$$dC^*_1/[(C^*_1)^4 + Q(C^*_1) - QC^*_T] = -k_{1n}dt. \quad (12)$$

With general biquadratic expressions, we redefine the following quantities:

$$A = \frac{Q^2}{2} + \left(\frac{Q^4}{4} + \frac{(4QC^*_T)^3}{27}\right)^{1/2},$$

$$B = \frac{Q^2}{2} - \left(\frac{Q^4}{4} + \frac{(4QC^*_T)^3}{27}\right)^{1/2},$$

$$p = A^{1/3} + B^{1/3}, \qquad E = P^{1/2}, \qquad f = 2QP^{-1/2}.$$

Eq. (12) takes the following form, letting $C = C^*_{1(t)}$:

$$x^4 - Qx - QC^*_T = (x^2 - Ex + P/2 + f)(x^2 + Ex + P/2 - f),$$

using a partial fractional procedure, this expression becomes

$$\frac{1}{x^4 - Qx - QC^*_T} = \frac{ax+b}{x^2 - Ex + P/2 - f} + \frac{ex+d}{x^2 + Ex - P/2 - f}. \quad (13)$$

The quantities a, b, c and d are evaluated from eq. (13). The general expression of eq. (12) then becomes

$$(c/2)\log(x^2 + Ex + P/2 - f) + \frac{cE/2 - d}{[E^2 - 2(P-2f)]^{1/2}} \times \log\left(\frac{[E^2 - 2(P-2f)]^{1/2} + E + 2x}{[E^2 - 2(P-2f)]^{1/2} - E - 2x}\right) + (a/2)\log(x^2 - Ex + P/2 + f) \times \frac{2(aE/2+b)}{[2(P+2f) - E^2]^{1/2}}\tan^{-1}\left(\frac{2x-E}{[2(P+2f)-E^2]^{1/2}}\right) = -k_{n1}t + k_0. \quad (14)$$

The term $C^*_{1(t)}$ can be evaluated by iteration [29] and k_0 evaluated under the two initial conditions by:

(i): $t = 0$, $C^*_{1(t)} = 0$

$$k_0 = (c/2)\log|P/2 - f| + \frac{cE/2 - d}{[E^2 - 2(P-2f)]^{1/2}}\log\left(\frac{[E^2 - 2(P-2f)]^{1/2} + E}{[E^2 - 2(P-2f)]^{1/2} - E}\right) + (a/2)\log|p/2 + f| + \frac{2(aE/2+b)}{[2(P+2f) - E^2]^{1/2}} \times \tan^{-1}\left(\frac{-E}{[2(P+2f)-E^2]^{1/2}}\right). \quad (15)$$

(ii): $t = 0$, $C^*_{1(t)} = C^*_T$

$$k_0 = (c/2)\log\{(C^*_T)^2 + EC^*_T + P/2 - f\} + \frac{cE/2 - d}{[E^2 - 2(P-2f)]^{1/2}} \times \log\left(\frac{[E^2 - 2(P-2f)]^{1/2} + E + 2C^*_T}{[E^2 - 2(P-2f)]^{1/2} - E - 2C^*_T}\right)$$

$$+ (a/2)\log\{(C_T^*)^2 - EC_T^* + P/2 + f\}$$

$$+ \frac{2(aE/2 + b)}{[2(P + 2f) - E^2]^{1/2}} \tan^{-1}\left(\frac{2C_T^* - E}{[2(P + 2f) - E^2]^{1/2}}\right). \quad (16)$$

Since C_1^* and C_i^* can be computed from eqs. (5)–(16), and C_1^{**} and C_i^{**} can be evaluated from the subsequent expressions (17)–(23). K_{app}, as defined in section 2 [15] can be obtained as a function of the column length. Let us note that these kinetic expressions can be applied directly to our simultation with both species A* and A_n^* present initially because the distribution evolving from the initial weight fraction of monomer f_1 of the A* molecule is assumed to overlap with that from the weight fractions of f_i of A_n^* molecules, so that both monomer and n-mer reach equilibrium concentration at every point along the column. Actually, this is not the case, due to variation of the kinetic rate with the distribution of $C_{1(t)}^*$.

The reverse and forward equilibration rate constants of species k_{ii} and k_{-ii} for monomer have their usual significance in the mobile phase, dictating the finite local equilibration rate which will perturb the overall boundary profiles of the system. The effects of kinetically-controlled local equilibration in either the mobile or stationary phase must be considered in evaluating the elution boundary profiles. Thus, the rate of k_{ii} and k_{-i_i} between mobile and stationary phases, as shown in the fig. 1, will affect the differential equations which follow.

i) $n = 1$, isomerization

$$\partial C_1^{**}/\partial t = -k_{11}C_1^{**} + k_{-11}C_1^*,$$
$$\partial C_{1a}^{**}/\partial t = -\tilde{k}_{11}C_{1a}^{**} + \tilde{k}_{-11}C_{1a}^{**}, \quad (17)$$

where $\tilde{k}_{11}$ and $\tilde{k}_{-11}$ denote the exchange rates between mobile and stationary phases of the isomer.

This expression, then, describes the stationary phase much as its counterpart, eq. (3), describes the mobile phase. $\tilde{k}_{ii}$ is the isomerization rate constant between the stationary and mobile phases.

ii) $n = 2$, monomer–dimer system:

$$\partial C_1^{**}/\partial t = -k_{11}C_1^{**} + k_{-11}C_1^*,$$
$$\partial C_2^{**}/\partial t = -k_{22}C_2^{**} + k_{-22}C_2^*. \quad (18)$$

iii) $n = 3$, monomer–trimer system

$$\partial C_1^{**}/\partial t = -k_{11}C_1^{**} + k_{-11}C_1^*,$$
$$\partial C_3^{**}/\partial t = -k_{33}C_3^{**} + k_{-33}C_3^*. \quad (19)$$

iv) $n = 4$, monomer–tetramer system:

$$\partial C_1^{**}/\partial t = -k_{11}C_1^{**} + k_{-11}C_1^*,$$
$$\partial C_4^{**}/\partial t = -k_{44}C_4^{**} + k_{-44}C_4^*. \quad (20)$$

Letting $C_{1(t)}^*$ equal the concentration of monomer in the mobile phase at time t, solving equations (17) through (20) for $C_{i(t+\Delta t)}^{**}$ yields $C_{i(t)}^*$ and $C_{i(t)}^{**}$ at time t between the stationary and mobile phases:

$$C_{i(t+\Delta t)}^{**} = \left\{\frac{1}{(k_{ii} + k_{-ii})}\,[k_{ii}C_{i(t)}^{**} - k_{ii}C_{i(t)}^*]\exp\{-(k_{ii} + k_{-ii})\Delta t\} + \frac{k_{-ii}}{k_{ii} + k_{-ii}}[C_{i(t)}^{**} + C_{i(t)}^*]\right\}, \quad i = 1, 2, \ldots, n. \quad (21)$$

The concentrations of $C_{1(t+\Delta t)}^{**}$ is

$$C_{1(t+\Delta t)}^{**} = \left\{\frac{1}{k_{11} + k_{-11}}\,[k_{11}C_{1(t)}^{**} - k_{-11}C_{1(t)}^*]\exp\{-(k_{11} + k_{-11})\Delta t\} + \frac{k_{-11}}{k_{11} + k_{-11}}[C_{1(t)}^{**} + C_{1(t)}^*]\right\}. \quad (22)$$

In this case all k_{ii} and k_{-ii} are expressed in reciprocal minutes [15,31]. All the kinetic functions described to this point decrease monotonically with respect to $C_{1(t)}^*$. Thus, for simulation experiments of varying model systems in which all interacting molecules are initally confined to the boundary states we have described, one has only to measure the local equilibration at time t and compare with $C_{i(t)}^*$.

3. Simulation procedure on large-zone concentration gradient profiles

Our computer simulation procedure is based on the continuity equation (1) as described in the previous

Table 1
System parameters used in simulation (held constant)

Parameters	Monomer–dimer system	Monomer–tetramer system
Column length, l	10 cm	10 cm
Column cross-sectional area, A	1.0 cm^2	1.0 cm^2
Sephadex gel	G100R	G200R
Flow rate, F.	1.2 ml/hr	1.2 ml/hr
α, void volume/ℓ	0.295	0.295
β, internal volume/ℓ	0.670	0.670
Partition cross-section, ξ_i	$\xi_1 = 0.667$	$\xi_1 = 0.80$
	$\xi_2 = 0.500$	$\xi_4 = 0.64$
Partition coefficient, σ_i	$\sigma_1 = 0.571$	$\sigma_1 = 0.754$
	$\sigma_2 = 0.306$	$\sigma_4 = 0.515$
Initial concentration, C_0	0.1 mg/ml	0.1 mg/ml
Axial dispersion coefficient, L_i	$L_1 = 8.89 \times 10^{-4}$ cm^2/min	$L_1 = 3.61 \times 10^{-4}$ cm^2/min
	$L_2 = 5.66 \times 10^{-4}$ cm^2/min	$L_4 = 4.86 \times 10^{-4}$ cm^2/min
qd^2	5.4×10^{-6} cm^2	5.4×10^{-6} cm^2

q is a gel particle-packing factor, d is the gel particle diameter. A is the column cross-sectional area, $\xi_i = (\alpha + \beta\sigma_i)$. The rate of movement of the centroids is related to the partition cross-section, ξ, by $\xi = (F/A)(dt/d\bar{x})$.

paper [15]. The simulation methods to be compared were incorporated into programs written in Fortran and computation done on an Amdahl 470/6-2 IBM computer (a modification of the IBM 370). Concentration gradients were plotted with a Gould plotter as a function of the distance coordinate, x, varying the flow time and $C^*_{1(t)}$ and equilibrium constant as a function of the distance coordinate. All simulations were carried out to describe the large zone boundary undergoing rapid or slow equilibration, using the simulation parameters described by Zimmerman and Ackers [22] and by Chun and Yang [15].

4. Results and discussion

The time-course dependent simulation of monomer–dimer and monomer–tetramer systems, based on eq. (1), is shown in figs. 3a-d and figs. 4a-d. Simulation in figs. 3a-d was done on Sephadex G100R gel

Table 2
Weight fraction of monomer and kinetic parameters of k_{ij} and k_{ji} for monomer–dimer system after an elapsed time of 190 min.

Weight fractions monomer–dimer	k_{12} $(mg/ml)^{-1}$ min^{-1}	k_{21} $(min)^{-1}$	K_0 $(mg/ml)^{-1}$	overall process	gradient curves
90%–10%	1.230	1.00	1.23	rapid	A(a)
90%–10%	0.0123	0.01	1.23	slow	1(1)
75%–25%	4.440	1.00	4.44	rapid	B(b)
75%–25%	0.440	0.01	4.44	slow	2(2)
50%–50%	2.00	0.100	20.0	rapid	C(c)
50%–50%	0.02	0.001	20.0	slow	3(3)
25%–75%	120.0	1.00	120.0	rapid	D(d)
25%–75%	1.20	0.01	120.0	slow	4(4)

Kinetic parameters in examining the rate of equilibration between the mobile and stationary phases are: $k_{11} = 0.1$, $k_{-11} = 0.1$ (min^{-1}); $k_{22} = 0.1$, $k_{-22} = 0.05$ (min^{-1}). Gradient curves in the first column consider both the mobile and stationary phases. Gradient curves in the second column, indicated by parenthesis, consider only the mobile phase.

Table 3
Weight fraction of monomer and kinetic parameters of k_{ij} and k_{ji} for monomer–tetramer system after an elapsed time of 192 min

Weight fraction monomer, monomer–dimer	k_{14} (mg/ml)$^{-3}$ min^{-1}	k_{41} (min^{-1})	K_0 (mg/ml)$^{-3}$	overall process	gradient curves
90%–10%	152.00	1.00	152.0	rapid	A(a)
90%–10%	1.520	0.01	152.0	slow	1(1)
75%–25%	79.00	0.10	7.9×10^2	rapid	B(b)
75%–25%	0.79	0.01	7.9×10^2	slow	2(2)
50%–50%	80.0	0.010	8.0×10^3	rapid	C(c)
50%–50%	8.0	0.001	8.0×10^3	slow	3(3)
25%–75%	192.00	0.001	1.92×10^5	rapid	D(d)
25%–75%	1.920	1×10^{-5}	1.92×10^5	slow	4(4)

Kinetic parameters in examining the rate of equilibration between the mobile and stationary phases are: $k_{11} = 0.1$, $k_{-11} = 0.1$ (min^{-1}); $k_{44} = 0.1$, $k_{-44} = 0.02$ (min^{-1}). Gradient curves in the first column consider both the mobile and stationary phases. Gradient curves in the second column, indicated by parenthesis, consider only the mobile phase.

at a flow rate of 1.2 ml/hr. The diameter of the monomer is 17.5 Å and the running times for experiments at the flow rate were simulated to maintain a constant flow throughout the experiment. The axial dispersion coefficient of monomer, $L_1 = 8.89 \times 10^{-4}$ cm^2/min, as shown in table 1. The monomer is further assumed to form with a molecular radius of 17.5 Å and a diffusion coefficient of 8.97×10^{-7} cm^2/s. The term qd^2 relates the particle size and geometry to the average equilibration time between mobile and stationary phases of the column [22,28], and was calculated to be 5.4×10^{-6} cm^2. We assumed that system parameters such as L, F, ξ and A are independent of the column length, x_1, time, t, and initial concentration, C, as shown in table 1.

Simulation in figs. 4a-d was done on Sephadex G200R at a flow rate of 1.2 ml/hr. The axial dispersion coefficients of monomer and tetramer systems are shown in tables 2 and 3, respectively. The overall reaction rate of equilibration, whether rapid or slow, in each specific instance is indicated in these tables.

4.1. Analytical solution for the general kinetic expression for the concentration of monomer as a function of equilibration time, $C^*_{1(t)}$

To evaluate k_{ij} and k_{ji} (as shown in figs. 2a and b, for a given time as a function of the distance coordinate from the kinetic expression for the concentration of monomer, given in eq. (4), the procedure is as follows:

Initial boundary conditions of (i) $t = 0$, $C^*_{i(t)} = 0$ and (ii) $t = 0$, $C^*_{i(t)} = C^*_I$ are set for the various reaction systems to be studied (I through IV of eq. (4) as described in the text) in order to determine the kinetic properties of the $C^*_{1(t)}$ species, using eqs. (5), (6), (11a), (11b), (15) and (16). Given values of k_{ij} and k_{ji}, $C^*_{1(t)}$ can be predicted precisely as a function of the equilibration time, provided the composition of the weight fraction of monomer at the initial conditions is known, as shown in figs. 2a and b.

Thus, for a chosen set of kinetic parameters, it is possible to determine whether the reaction will proceed at a slow or rapid rate. It should be noted that the function $C^*_{1(t)}$, given values of k_{ij} and k_{ji}, is exponential with time for both rapid and slowly equilibrating systems [15]. When the weight fraction of the associating species reaches equilibrium composition, the magnitude of $t_{1/2}$ must be taken into consideration in any evaluation of the extent to which the reaction is kinetically controlled, since this kinetic effect varies with the distribution of each species along the column.

For a monomer–dimer system, as shown in fig. 2a, the kinetic parameters from table 2 used to generate the curve are:

(i) $t = 0$, $C^*_{1(t)} = 0$, for the 2′ region with $k_{12} = 120$, $k_{21} = 0.01$ and for 1′ with $k_{12} = 1.20$, $k_{21} = 0.01$.
(ii) $t = 0$, $C^*_{1(t)} = C^*_T$, for the 2 region with $k_{21} = 1.20$, $k_{21} = 0.01$ and for 1 with $k_{12} = 1.20$, $k_{21} = 1.0$.

For a monomer–tetramer system, as shown in figs.

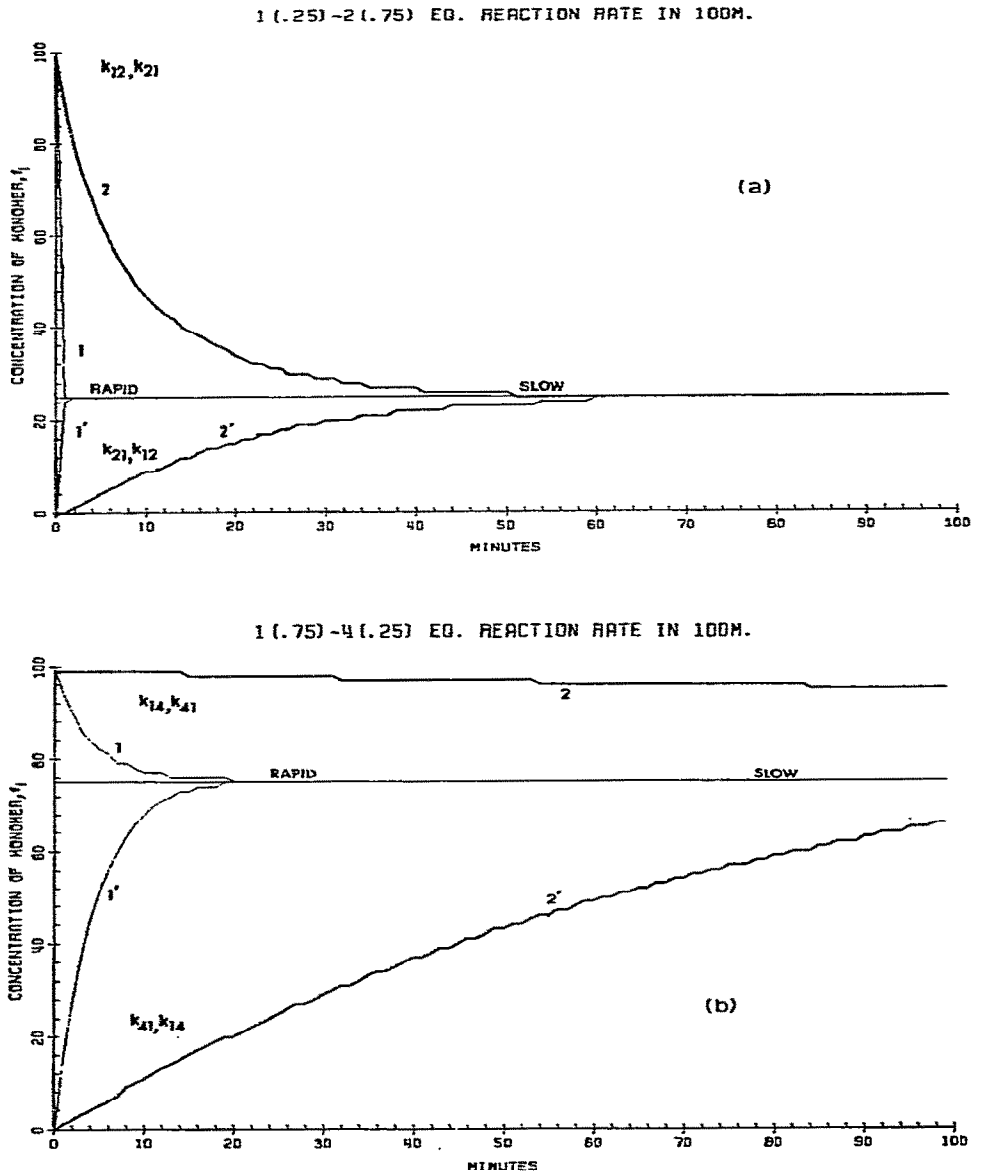

Fig. 2. Theoretical distribution of the weight fraction of monomer in the mobile phase of a system undergoing (a) 25 : 75% monomer–dimer association after an elapsed time of 100 min on Sephadex G100R gel, and (b) 75 : 25% monomer–tetramer association after an elapsed time of 100 min on Sephadex G200R gel. 1 and 1' represent rapidly equilibrating systems; 2 and 2' cases of slow equilibration.

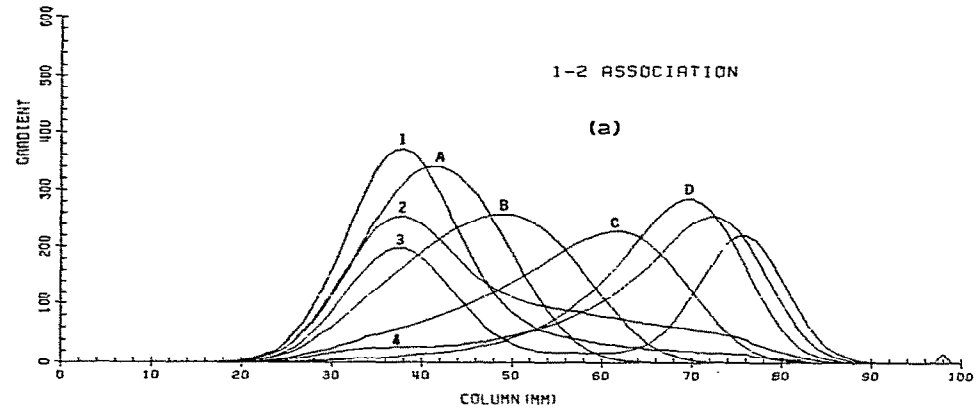
1-2 ASSOCIATION
(a)
GRADIENT
COLUMN (MM)
1
A
2
B
3
C
D
4

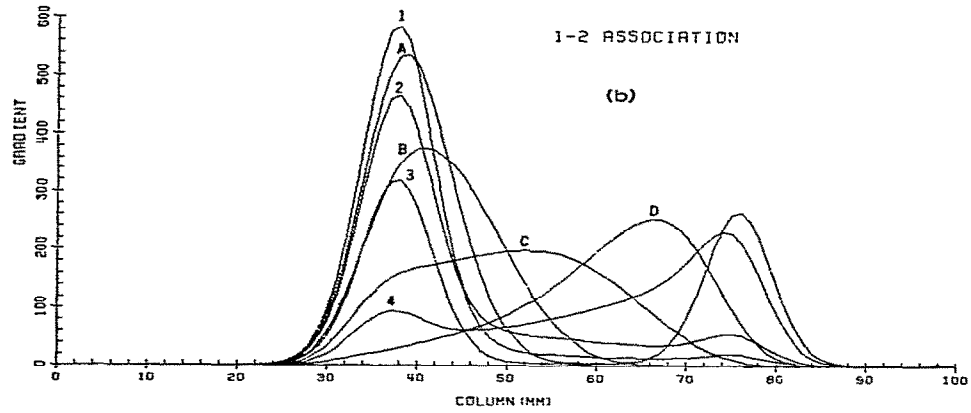
1-2 ASSOCIATION
(b)
GRADIENT
COLUMN (MM)
1
A
2
B
3
C
D
4

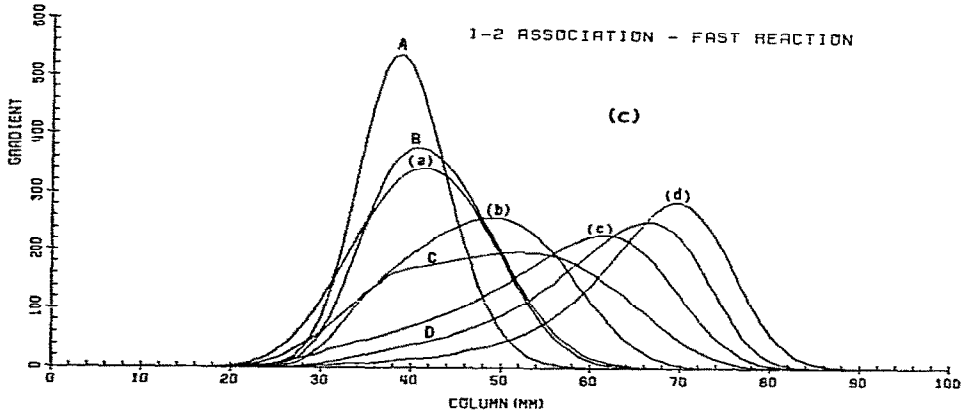
1-2 ASSOCIATION - FAST REACTION
(c)
GRADIENT
COLUMN (MM)
A
B
(a)
(b)
(c)
(d)
C
D

Fig. 3a, b, c.

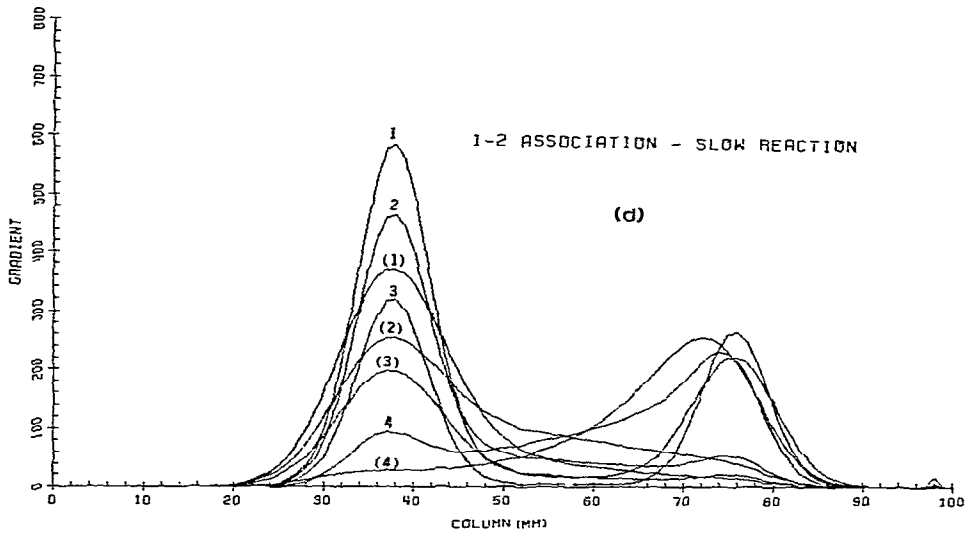

Fig. 3. The time-course dependent simulation of a monomer–dimer system undergoing rapid and slow equilibration (a) in the mobile phase, on Sephadex G200R gel, and (b) in both the mobile and stationary phases. (c,d) A comparison of rapid (c) respectively slow (d) equilibration in the mobile phase alone and rapid (c), respectively slow (d) equilibration in both the mobile and stationary phases of a system undergoing monomer–dimer association, as influenced by k_{ij} and k_{-ij}. The weight fraction of monomer and kinetic parameters are given in table 2.

2b, the kinetic parameters from table 3 used to generate the curve are

(i) $t = 0$, $C^*_{1(t)} = 0$, for the 2′ region with $k_{14} = 0.79$, $k_{41} = 0.01$, and for 1′ with $k_{14} = 79.0$, $k_{41} = 0.10$.
(ii) $t = 0$, $C^*_{1(t)} = C^*_T$, for the 2 region with $k_{14} = 0.79$, $k_{41} = 0.01$, and for 1 with $k_{14} = 79.0$, $k_{41} = 0.10$.

The distribution of $C^*_{1(t)}$ for a given time in the mobile phase may then be precisely evaluated for the various kinetic models we have proposed. The resulting $C^*_{1(t)}$ distributions are incorporated into the evaluation of C^{**}_1 in the stationary phase [15], as described in section 1. The distribution of $C^*_{1(t)}$ and $C^{**}_{1(t)}$ as a function of the distance coordinate are considered in the evaluation of the continuity equation (1), to determine the profile of several interacting species.

4.2. A monomer–dimer system undergoing rapid or slow equilibration in the mobile phase

Fig. 3a provides a comparison of slow and rapid equilibration in the mobile phase alone of a system undergoing monomer–dimer association. Those gradient curves marked by integers 1 through 4 represent a slow rate of equilibration and are easily distinguished by their bimodality from the curves of a rapid equilibrating system, designated A through D. Accompanying kinetic parameters for eq. (1) are given in table 2. The degree of bimodality shown in these reaction boundaries varies with the value of k_{12} (k_{ij}), while k_{21} (k_{ji}) seems to have little effect on the nature of the gradient curve, beyond contributing to a slight variation of the leading boundary position.

In contrast, in the case of rapid equilibration, k_{21} (k_{ji}), the reverse kinetic rate, seems to determine the unimodal character of the reaction boundary, while k_{12} (k_{ij}) determines the degree of skewing in the trailing edge of the boundary. The centroid position of the boundary profiles vary as a function of column length. These conclusions also hold true for cases of monomer–dimer association such as shown in fig. 3b, where both the mobile and stationary phases are considered.

4.3. Monomer–dimer system undergoing rapid equilibration between the mobile and stationary phases

A comparison of rapid equilibration in the mobile phase alone and rapid equilibration in the mobile and stationary phases of a system undergoing monomer–dimer association is shown in fig. 3c, with the accompanying kinetic parameters given in table 2. Despite wide variation in the kinetic parameters we considered, in comparing reaction boundaries for the mobile phase alone with those of the mobile and stationary phases, we found that the rate of chemical equilibration between mobile and stationary phases had no pronounced effect on the reaction boundary, although we observed a sharpening of the centroid position which we attribute to kinetic effects. Again, the reverse kinetic rate k_{ji} seems to be the principal determinant of the shape of the boundary profile for a rapidly equilibrating system.

4.4. Monomer–dimer system undergoing slow equilibration between the mobile and stationary phases

Fig. 3d shows a comparison of slow equilibration in the mobile phase alone and slow equilibration in the mobile and stationary phases of a system undergoing monomer–dimer association, varying the weight fractions and kinetic parameters as listed in table 2.

When the kinetic rate of equilibration between the mobile and stationary phases is considered, a distinct sharpening of the centroid position and increased separation of the leading boundary are observed, when compared with the boundary profiles of the mobile phase alone. Hence, for a system undergoing slow equilibration, the kinetic effects of the reverse rate constants k_{ii} and k_{-ii} are readily apparen Species distribution as a function of time, $C^{*}_{1(t)}$, varie much more widely along the column length in cases of slow equilibration, whether only the mobile or both mobile and stationary phases are considered.

On the whole, therefore, the effects of kinetic controls on a slow equilibration process are much more pronounced than in a rapidly equilibrating syste with the kinetically-controlled rate between the mobi and stationary phases serving as the principal determinant of boundary profile.

4.5. Kinetic controls on a monomer–tetramer system

Fig. 4a is a comparison of slow and rapid equilibration in the mobile phase alone of a system undergoing monomer–tetramer association in Sephadex G200R gel. The weight fractions of monomer and kinetic para eters k_{ij} and k_{ji} for such a system are given in table 3.

A hypersharp initial boundary was observed in all cases of slow equilibration. As k_{14} (k_{ij}), the forward kinetic rate, increases, it becomes increasingly difficul

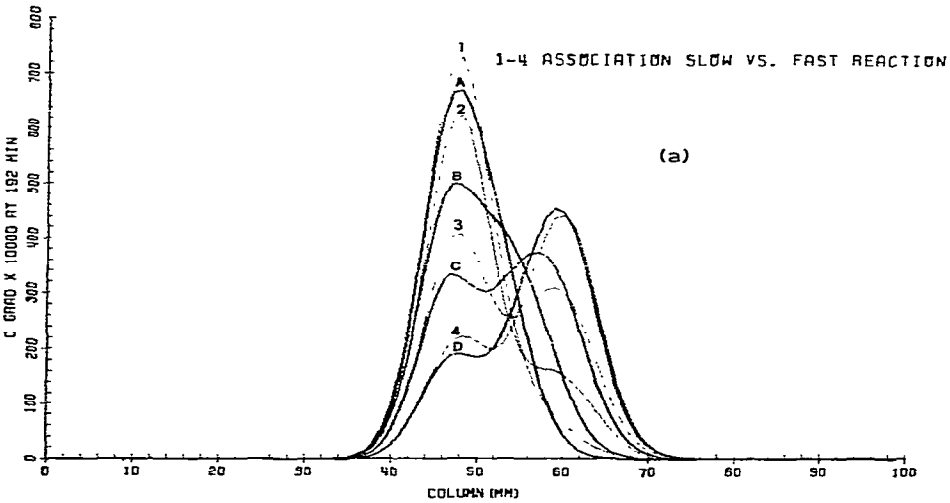

Fig. 4a.

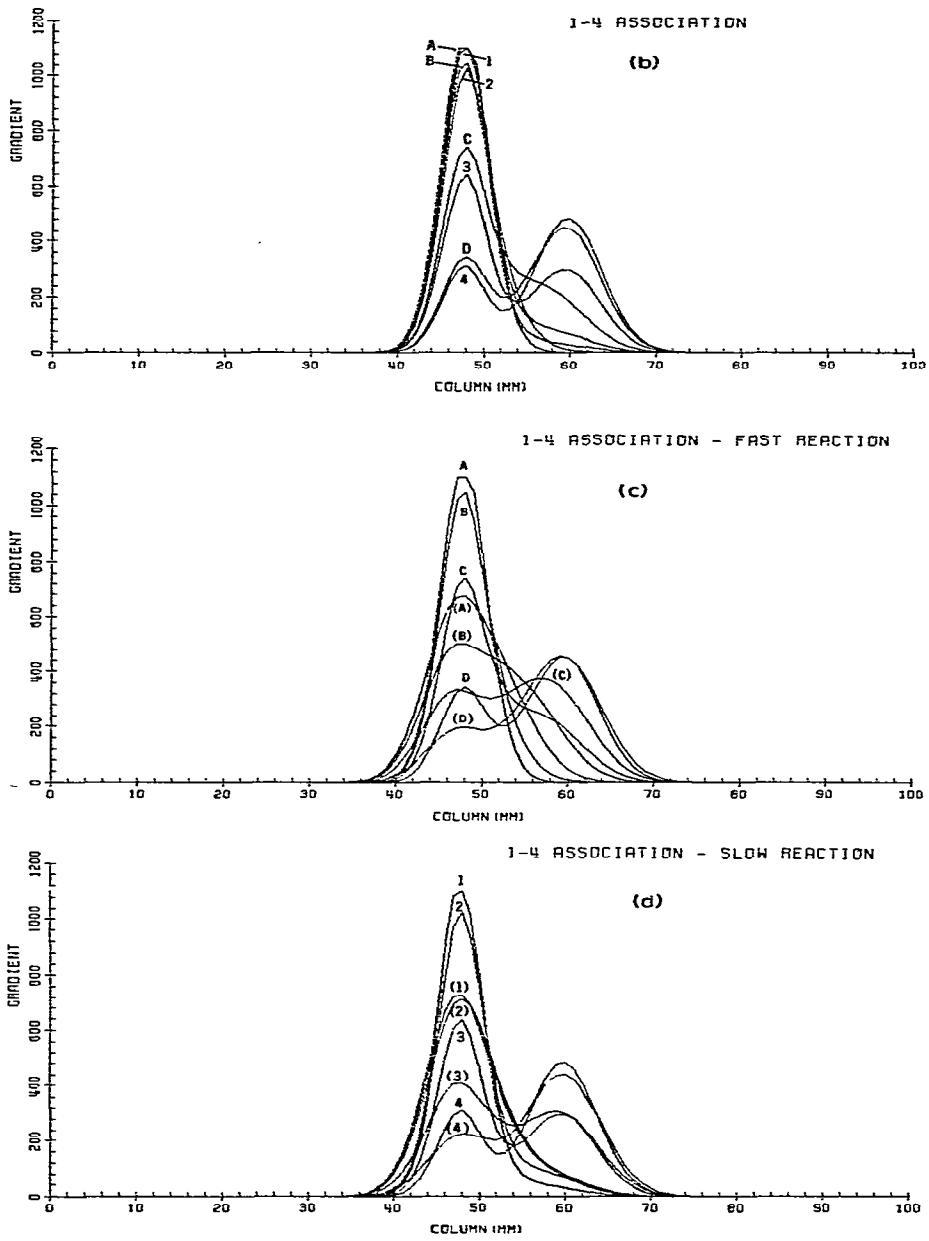

Fig. 4. The time-course dependent simulation of a monomer–tetramer system undergoing rapid and slow equilibration (a) in the mobile phase alone, on Sephadex G200R gel, and (b) between the mobile and stationary phases. (c,d) A comparison of rapid (c), respectively slow (d) equilibration in the mobile phase alone and rapid (c), respectively slow (d) equilibration in both the mobile and stationary phases of a system undergoing monomer–tetramer association. The weight fraction of monomer and kinetic parameters are given in table 3.

to distinguish between the boundary profiles of systems undergoing slow or rapid equilibration, noting that the reverse kinetic rate constant k_{41} (k_{ji}) decreases one hundred-fold over the range studied.

It appears that for a monomer–tetramer system such as this one, both kinetic parameters, k_{ij} and k_{ji}, play a principal role in determining the shape of the boundary profile.

When both rapid and slow equilibration between the mobile and stationary phases of a monomer–tetramer system are considered, as shown in fig. 4b, we note a considerable sharpening of both the leading and trailing boundaries, due to the effect of the kinetically-controlled constant k_{ii} and k_{-ii}. On the whole, however, the kinetic controls appear to be operating on the system similarly to those observed in fig. 4a. The maximum height of the peak position is reduced in rapid equilibration, accompanyed by a shift in the leading boundary, varying the composition of the weight fraction of monomer.

It appears that the kinetically-controlled rate between the mobile and stationary phase is, indeed,

Table 4
Concentration distributions, in the mobile phase and the stationary phase, as a function of distance coordinates for a monomer (25%)–dimer(75%) system undergoing slow equilibration at 190 min, where $k_{12} = 120$, $k_{21} = 0.01$.

Column length (mm)	$C_1^* \times 1000$ (mg/ml)	$C_1^{**} \times 1000$ (mg/ml)	$\log(K_{app}/K_0) \times 100$	Column length (mm)	$C_1^* \times 1000$ (mg/ml)	$C_1^{**} \times 1000$ (mg/ml)	$\log(K_{app}/K_0) \times 100$
0	0	0	0	55	104	108	−94
25	0	0	−199	56	107	112	−92
26	0	0	−200	57	111	115	−90
27	0	0	−205	58	114	119	−89
28	0	0	−206	59	118	123	−87
29	1	1	−207	60	121	126	−85
30	2	2	−205				
				61	125	130	−84
31	4	3	−201	62	128	134	−82
32	6	6	−198	63	132	138	−81
33	9	9	−194	64	136	142	−80
34	13	13	−190	65	140	146	−78
35	18	18	−185	66	144	150	−77
36	24	24	−180	67	147	154	−75
37	31	31	−174	68	151	158	−74
38	37	38	−168	69	155	161	−72
39	44	45	−161	70	159	165	−70
40	50	51	−155				
				71	163	169	−67
41	55	57	−148	72	163	172	−65
42	60	62	−142	73	170	175	−62
43	64	67	−136	74	173	177	−59
44	68	71	−130	75	176	180	−56
45	72	75	−125	76	179	181	−53
46	75	78	−121	77	181	183	−50
47	78	81	−116	78	182	184	−48
48	82	85	−113	79	183	184	−46
49	85	88	−109	80	184	185	−45
50	88	91	−106				
				81	185	185	−44
51	91	94	−103	82	185	185	−43
52	94	98	−101	83	185	185	−42
53	97	101	−98	99	185	185	−41
54	100	105	−96				

the principal determinant of the elution boundary profile in molecular sieve chromatography, with only a minimal dependence on axial dispersion.

Fig. 4c shows a monomer–tetramer system undergoing rapid equilibration in the mobile phase alone as well as between the mobile and stationary phases. Here, the distinct sharpening of the initial boundary peaks may be attributed to the kinetically-controlled rates constants k_{ii} and k_{-ii}. Consistent with our other findings, this kinetic effect is more pronounced in a monomer–tetramer system undergoing slow equilibration, as seen in fig. 3d. In the section which follows, we describe the simulation results for eq. (4), as adapted to our computer program [15], evaluating the general kinetic expression for the time-course dependent concentration of monomer, $C^{*}_{1(t)}$ and $C^{**}_{1(t)}$ in the mobile and stationary phases, as a function of the distance coordinate in a system undergoing slow or rapid equilibration.

4.6. $C^{*}_{1(t)}$ and $C^{**}_{1(t)}$ as a function of the distance coordinate in the mobile and stationary phase

Tables 4 and 5 show the concentration distributions, in the mobile and the stationary phase, as a function of the distance coordinate for monomer–dimer and monomer–tetramer systems, respectively. Since the column equilibrium is not always instantaneous, the apparent equilibrium constant may be evaluated from the expression:

$$K_{app} = (C_i^{*} + C_i^{**})/(C_1^{*} + C_1^{**})^{i}, \qquad K_0 = k_{1i}/k_{i1}. \tag{23}$$

The apparent equilibrium constants will vary with the distance coordinate. Note that the variation of the species distribution $C^{*}_{1(t)}$ for both these rapidly equilibrating systems is much greater in the mobile phase than is the distribution of $C^{**}_{1(t)}$ in the stationary

Table 5
Concentration distributions, in the mobile phase and the stationary phase, as a function of the distance coordinates, for a monomer(25%)–tetramer(75%) system undergoing slow equilibration at 192 min, where $k_{14} = 192.0$, $k_{41} = 0.001$.

Column length (mm)	$C_1^{*} \times 1000$ (mg/ml)	$C_1^{**} \times 1000$ (mg/ml)	$\log(K_{app}/K_0) \times 100$	Column length (mm)	$C_1^{*} \times 1000$ (mg/ml)	$C_1^{**} \times 1000$ (mg/ml)	$\log(K_{app}/K_0) \times 100$
30	0	0	0	53	139	139	−167
31	0	0	0	54	145	145	−152
32	0	0	0	55	149	150	−138
33	0	0	0	56	133	154	−125
34	0	0	0	57	157	157	−113
35	0	0	0	58	160	160	−102
36	0	0	1133	59	163	162	−93
37	0	0	958	60	165	164	−85
38	0	0	794	61	167	166	−79
39	0	0	639	62	168	167	−74
40	0	0	495	63	169	168	−69
41	0	0	362	64	170	169	−66
42	1	1	242	65	171	169	−64
43	3	3	134	66	171	169	−62
44	7	6	41	67	171	169	−61
45	14	13	−37	68	171	169	−61
46	26	25	−99	69	171	169	−60
47	42	41	−146	70	171	169	−60
48	62	62	−176	71	171	169	−60
49	83	84	−192	72	171	170	−60
50	103	103	−196	73	171	170	−60
51	118	118	−191	74	171	170	−60
52	130	131	−181	75	171	170	−60

phase. This is consistent with our previously reported finding that the chemical reaction rate in the mobile phase of a system undergoing rapid equilibration is the principal determinant of the elution boundary profile.

5. Conclusion

Our simulation studies in monomer–dimer and monomer–tetramer systems have indicated that in a slowly equilibrating system, the kinetic rate constants k_{ii} and k_{-ii} between the mobile and stationary phases contribute significantly to the overall gradient boundary profile. In contrast, in the rapidly equilibrating system, the kinetic parameters k_{ij} and k_{ji} in the mobile phase are the principal determinants of the reaction boundary. Although the kinetic effects of k_{ii} and k_{-ii} may be noted, their contribution to the overall boundary profile is minimal.

If, however, the reversible binding of the solute to the gel matrix in the stationary phase,

$$A^{**} + Gel \underset{k_{ff}}{\overset{k_{ss}}{\rightleftharpoons}} Gel - A^{**}$$

from fig. 1, is considered, the kinetic expressions for the solute distribution in the stationary phase must become

$$(dC_{ig}^{**}/dt) = -k_{ff}[C_{ig}^{**}] + k_{ss}[C_i^{**}]\,[C_g]$$

$$(dC_i^{**}/dt) = -k_{ss}[C_i^{**}]\,[C_g] + k_{ff}[C_{ig}^{**}]$$

where C_i^{**} denotes the solute concentration in the stationary phase, C_g is the concentration of gel and C_{ig}^{**} is the concentration of the complex, Gel-A**. Here it is assumed that C_g remains constant, or that the number of available binding sites on the gel is large.

When these values are incorporated into the general continuity expression, eq. (1), it would appear to offer the most realistic picture of the processes which actually occur in the interacting system, because it considers both kinetic controls and the effects of solute binding to the gel on the system. The chief limitation of such a model is that it cannot make clear, in considering an actual interacting system, whether the associating species binds to the gel or whether these molecules in fact undergo association within the gel matrix.

Hence we must conclude that the most exciting computer simulation of interacting systems in molecular sieve chromatography must consider both the variation in $C_{1(i)}^{*}$ and $C_{1(i)}^{**}$ as a function of the distance coordinate in the mobile and stationary phase and the possible effects of interaction between solute and gel in the stationary phase. The degree to which such solute–gel interaction influences the concentration of monomer remains to be determined, and will be discussed at length in a succeeding paper.

References

[1] E.E. Brumbaugh and G.K. Ackers, J. Biol. Chem. 244 (1968) 6315.
[2] E.E. Brumbaugh and G.K. Ackers, Anal. Biochem. 41 (1971) 543.
[3] G.K. Ackers, in: Advances in protein chemistry, Vol. 24 (Acad. Press, 1970) p. 343, eds. C.B. Anfinsen, J.T. Edsall and F.M. Richards.
[4] M.M. Jones, G.A. Harvey and G.K. Ackers, Biophys. Chem. 5 (1976) 327.
[5] M.M. Jones, G.A. Harvey and G.K. Ackers, Biophys. Chem. 5 (1976) 339.
[6] B.B. Brown and J.K. Zimmerman, Biophys. Chem. 5 (1976) 351.
[7] L.P. Vickers and G.K. Ackers, Biophys. Chem. 6 (1977) 299.
[8] G.K. Ackers, E.E. Brumbaugh, S.H.C. Ip and H.R. Halvorson, Biophys. Chem. 4 (1976) 171.
[9] D.J. Cox, in: Methods in enzymology, eds. C.H.W. Hirs and S. Timasheff, in press (1977).
[10] J.R. Cann and W.B. Goad, J. Biol. Chem. 240 (1965) 148.
[11] W.B. Goad and J.R. Cann, Ann. N.Y. Acad. Sci. 164 (1969) 148.
[12] M. Dishon, G.H. Weiss and D.A. Yphantis, Biopolymers 4 (1966) 449.
[13] D.J. Cox, Arch. Biochem. Biophys. 119 (1967) 230.
[14] D.J. Cox, Arch. Biochem. Biophys. 129 (1969) 106.
[15] P.W. Chun and M.C.K. Yang, Biophys. Chem. 7 (1978) 347.
[16] D.I. Stimpson and J.R. Cann, Biophys. Chem. 7 (1977) 115.
[17] J.R. Cann and D.I. Stimpson 7 (1977) 103.
[18] R.M. Mitchell, Biopolymers 15 (1976) 1741.
[19] R.M. Mitchell, Biopolymers 15 (1976) 1717.
[20] H. Schönert, Biophys. Chem. 3 (1975) 161.
[21] J. Claverie and R. Cohen, Biopolymers 14 (1975) 1685.
[22] J.K. Zimmerman and G.K. Ackers, J. Biol. Chem. 246 (1971) 1078.
[23] J.K. Zimmerman and G.K. Ackers, J. Biol. Chem. 246 (1971) 7298.
[24] J.K. Zimmerman, D.J. Cox and G.K. Ackers, J. Biol. Chem. 246 (1971) 4242.

[25] J.K. Zimmerman, Biophys. Chem. 3 (1975) 339.
[26] J.K. Zimmerman, Biochem. 13 (1974) 384.
[27] H.R. Halvorson and G.K. Ackers, J. Biol. Chem. 249 (1974) 967.
[28] G.K. Ackers, The proteins, Vol. 1, eds. H. Neurath and R.L. Hill (Acad. Press, 3rd Edition, 1975) p. 1.
[29] H.H. Harmon, in: Modern factor analysis (2nd Edition, University of Chicago Press, 1967).
[30] P.W. Chun and Y.J. Yoon, Biopolymers 16 (1977) 2579.
[31] P.W. Chun, Biophys. Chem. 2 (1974) 170.